



Structural evolution of the thermal conversion products of modified coal tar pitch

Qi Li¹ · Dongyun Han¹ · Haiyan Qiao¹ · Weiwei Shi¹ · Yuqi Zhang¹ · Zubin Cao¹

Received: 8 April 2022 / Revised: 11 October 2022 / Accepted: 7 November 2022 / Published online: 1 December 2022
© The Author(s), under exclusive licence to Korean Carbon Society 2022

Abstract

Coal tar pitch is a product with high carbon content and aromatic compounds. Modified coal tar pitch is a high quality raw material for the preparation of intermediate phase pitch, needle coke, carbon microspheres, et al. In this paper, modified coal tar pitch was used as raw material, nitrogen was used as protective gas, and thermal conversion was carried out at constant temperatures (370, 390, 410, 420 °C). Polarized light microscopy, SEM, elemental analysis, FTIR spectroscopy, Raman spectroscopy and XRD diffraction combined with split-peak fitting were used to characterize the microstructures of the thermal transformation products. The results showed that the Iar and CH₃/CH₂ contents of the products increased with the gradual increase of the thermal conversion temperature, and the aromatic content increased. And the higher the temperature at the same heating rate, the more the ideal graphite microcrystal content, and the defective graphite microcrystals are converted into ideal graphite microcrystals during the thermal conversion process. When the reaction temperature exceeds 390 °C, the microstructure of the thermal transformation products is anisotropic spheres, and the small spheres fuse with each other and tend to be basin-like and mosaic structure as the temperature increases.

Keywords Modified coal tar pitch · Thermal conversion · Microstructure · Ethylene tar · Carbon material precursors

1 Introduction

Coal tar pitch (CTP) is the residual part of coal tar after distillation, which is abundant and cheap [1], but has low aromatic compound content and poor flowability. CTP is modified to form an aromatic structure by breaking the alkane side chains in the molecular structure, which can improve the aromatic content of pitch and can be used as a precursor for high-carbon materials such as carbon fiber and graphitized carbon [2–5]. MCTP-80 is CTP modified by ethylene tar and anthracene oil. The addition of ethylene tar and anthracene oil can improve the fluidity and aromatic content of CTP because ethylene tar and anthracene oil are rich in small-molecule aromatic compounds, which can effectively improve the properties of CTP and increasing its utilization value. But the quality of carbon material precursors prepared by adding additives modified by MCTP-80 only is unstable, mainly because the complex molecular structure

of MCTP-80 leads to excessive inverse activity and poor regularity of carbon microcrystal arrangement.

It was found that the key to the quality of carbon material precursors is the feedstock and processing conditions for thermal conversion [6–8]. The difference in the nature of the feedstock can lead to different structures of the thermal transformation products [9]. The molecular structure of CTP is complex and poorly mobile, and the reaction process is uncontrollable and the products are prone to coking only by thermal conversion treatment [10]. The modified MCTP-80 is rich in aromatic content and its own high plasticity, and then through thermal transformation can improve the reactivity of MCTP-80, increase the content of carbon microcrystals in the pitch system and can improve the stability. The aromatic structure of modified MCTP-80 is rich and its own plasticity is high, and then through the thermal transformation process can improve the reactivity of MCTP-80, increase the carbon content of the pitch system and can improve stability. During the thermal transformation reaction the defective carbon microcrystals in the molecular structure of MCTP-80 are transformed into ideal carbon microcrystals, which facilitates the formation of mosaic components in the microstructure of pitch. Zhao et al. [11] studied the

✉ Dongyun Han
hdy_mailbox@163.com

¹ College of Petroleum and Chemical Engineering, Liaoning Petrochemical University, Fushun 113000, China

thermal transformation behavior of ethylene residue pitch (ETP) and modified pitch (ETP obtained by atmospheric pressure air oxidation treatment) and found that the thermal stability, C=O and C–O content of the modified pitch were significantly higher than that of the ETP. During the thermal transformation process, the C=O functional group in the pitch molecule acts as the reactive site to induce the thermal transformation reaction. With the deepening of thermal transformation, the small molecule structure gradually polymerizes into a large molecule structure, and the carbon microcrystal arrangement of the pitch coke obtained from the thermal transformation of modified pitch is better than that of the pitch coke of modified pitch, and the thermostatic thermal transformation is more favorable to the formation of fibrous structure in the product. Zhu et al. [12] investigated the structural changes of refined coal bitumen at different thermal transformation temperatures using FTIR spectroscopy and split-peak fitting. With the increase of thermal conversion temperature, the aromatic index of refined coal bitumen becomes larger, which indicates that the refined coal bitumen induces aromatic ring enlargement during the thermal conversion process, and the reaction temperature is after 400 °C, the thick ring macromolecule compound undergoes violent polymerization reaction. Considered together, it is necessary to modify coal tar pitch for the preparation of high-quality carbon materials as precursors, and then to conduct thermal conversion studies.

In this paper, a modified coal tar pitch (MCTP-80) is used as raw material. The thermal conversion reaction of MCTP-80 was carried out in a tube furnace to discuss the effect of reaction temperature on the thermal conversion products of MCTP-80. The microstructures of the thermal transformation products were characterized by elemental analysis, FTIR spectroscopy, polarized light microscopy, XRD diffraction, Raman spectroscopy and SEM. It provides some theoretical basis for the preparation of high-quality carbon material precursors.

2 Experiment

2.1 Raw materials and reagents

Experimental raw materials: CTP from Yulin Tianxiao Chemical Group Co. Ethylene tar and anthracene oil from Fushun No. 2 plant.

Experimental reagents: quinoline and toluene from Sinopharm Chemical Reagent Co.

2.2 Preparation of MCTP-80

According to our previous study, CTP, ethylene tar and anthracene oil were blended and modified in the ratio of

8:1:1 by mass using the additive-polymerization method, and the resulting modified coal tar pitch was named MCTP-80.

2.3 Thermal conversion study of MCTP-80

Take 10 g of MCTP-80 sample and grind it into small particles into a 10 mL porcelain crucible, and heat it to 300 °C in a tube furnace at a heating rate of 5 °C/min using the purging method. When the temperature exceeds 300 °C, adjust the heating rate and heat the reactor to 370, 390, 410 and 420 °C, respectively, with a heating rate of 2 °C/min and keep the reaction at a constant temperature for 3 h. The products obtained by thermal transformation were named as MCTP-80-370, MCTP-80-390, MCTP-80-410 and MCTP-80-420, and the microstructures of all the thermal transformation products were analyzed.

2.4 Characterization methods

2.4.1 Property determination

The properties of softening point (SP), toluene insolubility (TI), quinoline insoluble matter (QI), coking value (CV) and Ash were determined for MCTP-80 and thermal transformation products according to national standards (GB/T 4507-1999, GB/T 2292-1997, GB/T 2293-1997, GB/T 8727-2008, GB/T 212-2008).

2.4.2 Elemental analysis

The content of C, H, N and S in the samples was determined by the elemental analyzer EA3000 produced by EuroVector, Italy, and the content of O in the samples was determined by the differential subtraction method.

2.4.3 FTIR spectroscopy measurements

A Nicolet Model 360 FTIR spectrometer was selected for the determination of MCTP-80 and thermal transformation products. The samples were ground into powder in a vessel, respectively, and mixed well with dried and treated pure KBr, in a ratio of 1:100, and pressed into slices at a pressure of 10 kg. The resulting slices were placed in the scanning area and then the determination analysis was started, where the determination scan range was 400–4000 cm⁻¹.

2.4.4 Optical microstructure and morphology analysis

The microstructures of MCTP-80 and thermal transformation products were characterized using an OLYMPUS BX51-P polarized light microscope manufactured by Olympus, Japan. Suitable samples were selected and placed into plastic molds, epoxy resin was poured and

cured at 60 °C. After cooling, the samples embedded in plastic molds were sanded step by step using different sizes of sandpaper (500#, 1000#, 2500#, 5000#) until there were a few tiny scratches on the surface, and then polished with a polisher until their sample surfaces were mirror-like, and the samples were observed under a polarized dark field.

The morphology of the thermal transformation products was observed using a scanning electron microscope (ΣIGMA-HD, Carl Zeiss, Germany).

2.4.5 Raman analysis

MCTP-80 and thermal transformation products were analyzed using a DXR-type Raman spectrometer from Thermo Fisher, USA. To further understand the content of different defects in the carbon microcrystalline structure of the samples, the analysis was performed mainly by D and G characteristic peaks and combined with curve fitting [13, 14] to determine the attribution of bands in the Raman spectra according to the literature [15].

2.4.6 XRD analysis

The samples were ground to a particle size below 325 mesh and analyzed on an x-ray polycrystalline powder diffractometer manufactured by Bruker D8 Advance, Germany, in the range of 2θ (resolution 0.02°) with diffraction angles from 10° to 90°, spectra and combined with curve fitting [16, 17] to analyze the carbon microcrystal particle size of MCTP-80 and thermal transformation products.

Table 1 Sample property determination

| Sample | SP/°C | TI/% | QI/% | CVI/% | Ash% |
|-------------|-------|-------|-------|-------|-------|
| MCTP-80 | 148 | 20.57 | 3.05 | 32.76 | 0.440 |
| MCTP-80-370 | 163 | 24.80 | 4.72 | 37.44 | 0.443 |
| MCTP-80-390 | 185 | 30.14 | 7.61 | 44.34 | 0.445 |
| MCTP-80-410 | 209 | 36.46 | 12.45 | 53.86 | 0.446 |
| MCTP-80-420 | 248 | 45.52 | 21.73 | 69.51 | 0.448 |

Table 2 Elemental composition of the samples

| Sample | C | H | N | S | O | C/H ^a |
|-------------|--------|-------|-------|-------|-------|------------------|
| MCTP-80 | 87.068 | 6.329 | 0.951 | 0.486 | 5.166 | 1.14 |
| MCTP-80-370 | 88.586 | 5.451 | 0.880 | 0.473 | 4.610 | 1.35 |
| MCTP-80-390 | 89.637 | 4.107 | 0.802 | 0.429 | 5.025 | 1.81 |
| MCTP-80-410 | 91.135 | 3.542 | 0.758 | 0.409 | 4.156 | 2.14 |
| MCTP-80-420 | 93.109 | 2.157 | 0.664 | 0.387 | 3.683 | 3.59 |

^aAtomic ratio of C and H

3 Results and discussion

3.1 Property analysis and elemental analysis of MCTP-80 and thermal transformation products

The results of the basic properties of MCTP-80 and thermal transformation products can be seen in Tables 1 and 2.

The analysis of the properties in Table 1 shows that with the increase of the thermal transformation temperature from 370 °C to 420 °C and the increase of the SP from 148 °C to 248 °C, the highest content of TI, QI and CV was observed for the thermal transformation product MCTP-80-420 at 420 °C. This indicates that the thermal conversion temperature has a significant contribution to the polymerization reaction between pitch molecules, and the small molecule compounds in the system gradually become larger into large molecule compounds as the thermal conversion temperature increases. The increasing trend of the indicators of pitch was flat until 400 °C, indicating that the polymerization reaction of MCTP-80 was not particularly violent at lower temperatures. When the reaction temperature reached 410 °C, the properties increased significantly, indicating that when the thermal transformation temperature exceeded 400 °C, the polymerization reaction deepened and the molecules in the MCTP-80 system underwent violent movements, thus increasing the content of molecular compounds.

Table 2 shows the results of the content of each element in MCTP-80 and thermal transformation products at different temperatures. As can be seen from the table, the C, H and O contents changed significantly, while the N and S contents changed more flatly, indicating that the polymerization reaction had a greater effect on the C, H and O elements [18]. With the increase of reaction temperature, the content of C elements increases, while the content of H, O, N and S decreases, which is due to the condensation of ethylene tar in MCTP-80 and short-ring aromatic hydrocarbons in anthracene oil into thick-ring aromatic hydrocarbons. During the cross-linking reaction between molecules in the polymerization process, carbon radicals attack other atoms and remove other heteroatoms in MCTP-80, resulting in an increase in C content and a decrease in the content of other elements,

which is the reason for the increase in the C/H atom ratio. Among them, the C/H atomic ratio is an important indicator to characterize the chemical structure of MCTP-80 and thermal transformation products. The larger the value of C/H atomic ratio, the more ring structure in the system, especially the increase of aromatic ring content [19, 20], which is also more favorable to the formation of carbon materials (Fig. 1).

3.2 Microstructure of MCTP-80 and thermal transformation products

MCTP-80 was thermally transformed and the product showed anisotropic structure under polarized light microscopy. However, the content and shape of each microscopic component of the thermal transformation products vary greatly at different temperatures. The distribution of polarized microstructures is shown in Fig. 2. MCTP-80 can be seen to be isotropic in the system under polarized light. When the thermal transformation temperature is 370 °C, anisotropic small spheres appear in the pitch system. However, most of the products were still isotropic pitches, and only a few apparently anisotropic spheres were generated, indicating that the aromatic ring structure in the system was not greatly condensed at this time. At the thermal transformation temperature of 390 °C, a large number of anisotropic spheres were formed in MCTP-80-390, and the anisotropic spheres were evenly distributed in the system, and also accompanied by an increase in the content of intermediate phase microcrystals, except for a few large anisotropic spheres formed, the size of the spheres in the system was basically the same, suggest that the molecules in the MCTP-80 thermal transformation product system grow in essentially the same way. The anisotropic spheres in MCTP-80-410 started to melt, and the content of intermediate-phase microcrystals

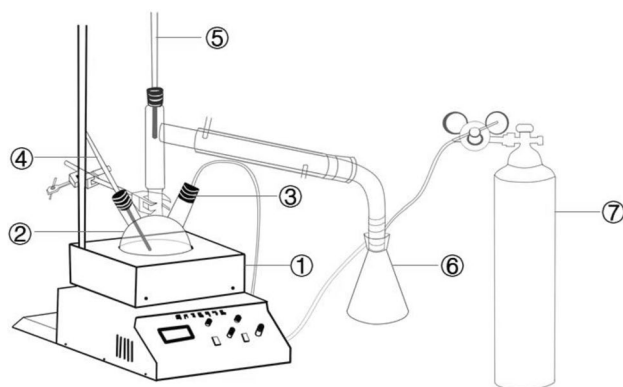


Fig. 1 Flow chart of modification experiment (① Stirring and temperature-controlled heating jacket ② Three flasks ③ Bubbler ④ Liquid phase thermometer ⑤ Gas phase thermometer ⑥ Light component effluent ⑦ Nitrogen cylinder)

increased. It was found that if the thermal transition temperature is too high, the molecular structure in the system starts to condense violently and tends to scorch. When the thermal transformation temperature is 420 °C, MCTP-80-420 shows the coexistence of basin-like and mosaic-like structures, accompanied by the formation of semi-coke lamellar structure and poor flowability of the product. It means that the thermal transformation temperature is too high at this time, and a large number of light components in the sample will escape from the system along with the process of temperature increase, and the anisotropic spheres generated during the thermal transformation process will form basin mosaic components under the action of gas shear force. Therefore, a thermal conversion temperature between 390 and 420 °C is suitable for the formation of high-quality carbon materials.

The evolution of the MCTP-80 thermal transformation product was initially determined by the polarized light microstructure. To further clarify the microscopic component content of the MCTP-80 thermal transformation product, the following quantitative analysis is required.

3.3 Changes in Iar and CH₃/CH₂ of MCTP-80 and thermal transformation products

The aromaticity index (Iar) and branched chain index (CH₃/CH₂) of MCTP-80 and thermal conversion products were calculated using FTIR and mathematical methods of split-peak fitting [21]. Figure 3a shows the FTIR spectra of the samples. It can be seen that the aromatic hydrogen at wave number 900–700 cm⁻¹, the number and position of bending vibration substitutions in the C-H plane on the aromatic ring at wave number 1300–900 cm⁻¹ and the wave number at C=C stretching vibration of the aromatic ring at wave number 1600–1350 cm⁻¹ have obvious absorption, except for the difference in intensity, the positions of the absorption peaks are basically the same, indicating that they have the same functional groups. The products with wave numbers around 3000 cm⁻¹ all have strong absorption peaks, which are caused by aromatic C-H stretching vibrations, at 2925 cm⁻¹ and 2850 cm⁻¹ indicate the intensity of the fat C-H absorption peak, if the absorption peak here is strong indicates less aromaticity and contains more CH₂ structure. And as the thermal transformation temperature increases, the intensity of the fat C-H absorption peak decreases and the aromaticity becomes larger. It indicates that the degree of polymerization intensifies with the increase of thermal transformation temperature, and the aliphatic hydrocarbon structure gradually changes to an aromatic ring structure. To further analyze the differences in the chemical structure of the thermal conversion product pitch, the samples were judged by calculating the Iar and the CH₃/CH₂. Iar is an indicator to characterize the degree of aromatic condensation of the product, and CH₃/CH₂ is used to determine the

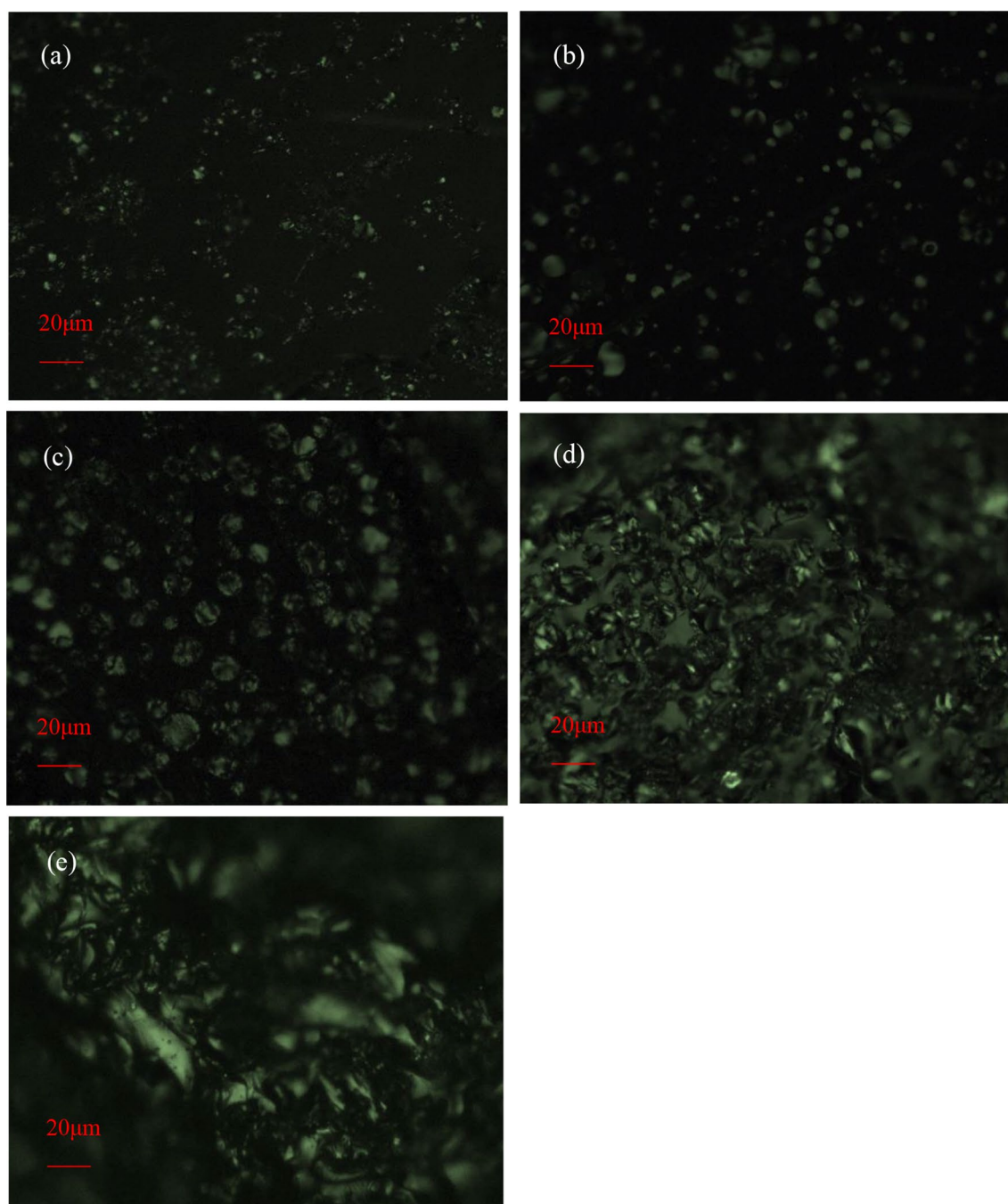


Fig. 2 Polarized micrographs (a) MCTP-80 (b) MCTP-80-370 (c) MCTP-80-390 (d) MCTP-80-410 (e) MCTP-80-420

degree of aromatic branching. A split-peak fit analysis was performed in the range of $3500\text{--}2800\text{ cm}^{-1}$ according to the literature [22–24], and Fig. 3b and c shows the curve fit, and the Iar and the CH_3/CH_2 were calculated according to Eqs. (1) and (2) [9, 22].

$$\text{Iar} = \text{Abs } 3050\text{ cm}^{-1} / (\text{Abs } 3050\text{ cm}^{-1} + \text{Abs } 2920\text{ cm}^{-1}), \quad (1)$$

$$\text{CH}_3/\text{CH}_2 = \text{Abs } 2950\text{ cm}^{-1} / \text{Abs } 2920\text{ cm}^{-1}. \quad (2)$$

The calculated equations $\text{Abs } 3050\text{ cm}^{-1}$, $\text{Abs } 2950\text{ cm}^{-1}$ and $\text{Abs } 2920\text{ cm}^{-1}$ represent the integrated area of absorbance of the fitted curves for peaks near 3050 , 2950 and 2920 cm^{-1} , respectively. Figure 3d shows the results of Iar and CH_3/CH_2 , which can be calculated by equation to obtain 0.09, 0.14, 0.27, 0.34, 0.38 for MCTP-80 and thermal

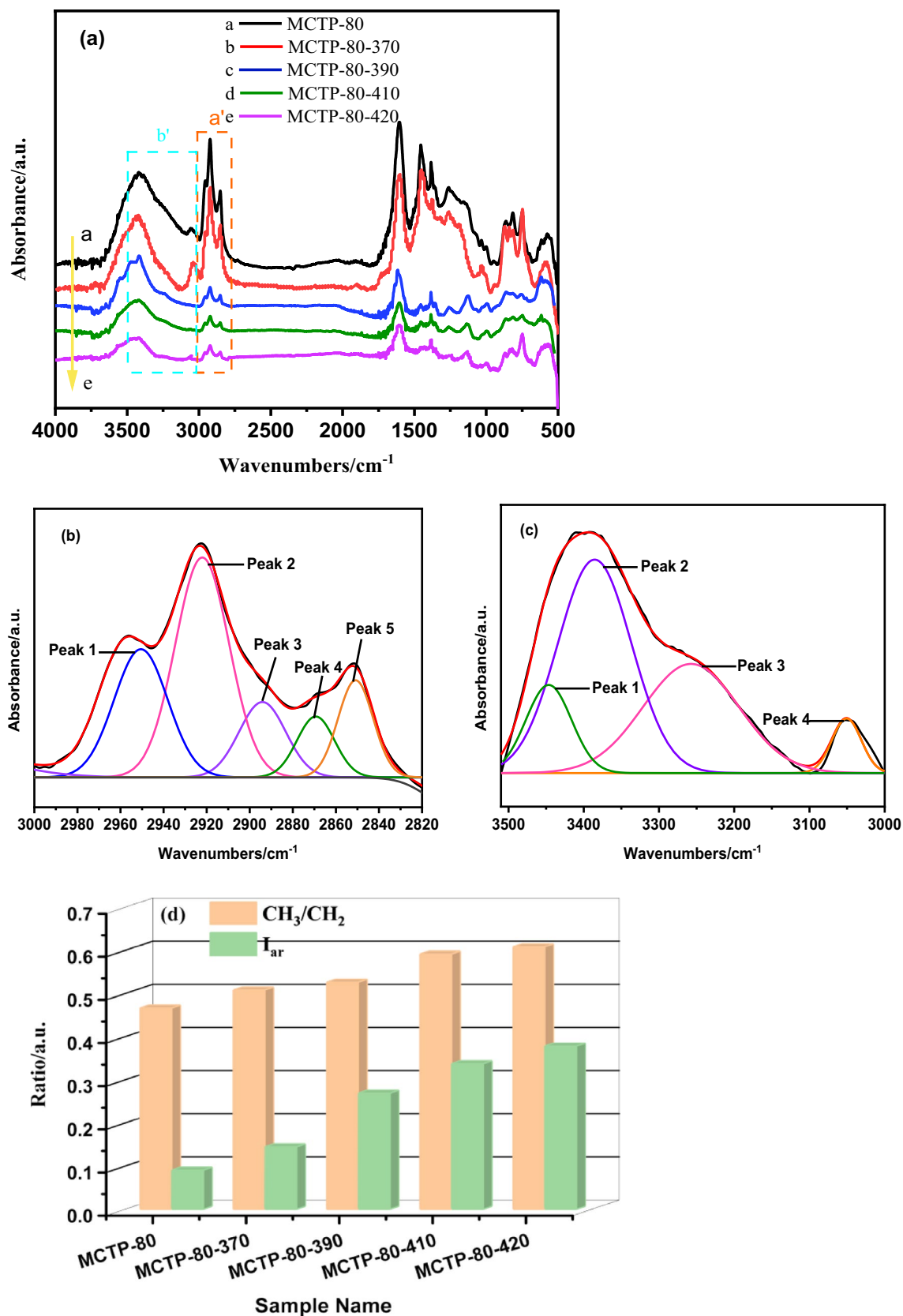


Fig. 3 a Infrared spectra of samples (b) curve fit of MCTP-80 in the a' segment (c) curve fit of MCTP-80 in the b' segment (d) calculated values of Iar and CH₃/CH₂ for MCTP-80 and thermal conversion products

conversion products Iar, and 0.47, 0.50, 0.52, 0.59, 0.61 for CH_3/CH_2 , respectively. This indicates that as the thermal transformation temperature increases, the molecular polymerization deepens and the aromatic index and content becomes more. The increase in CH_3/CH_2 indicates a decrease in the number of branched chains in the molecule, which is mainly attributed to the enhancement of the active reactive site. The molecular structure of MCTP-80 contains alkane side chains, and the reaction process is dominated by the cleavage of aliphatic chains and the polymerization of aromatic groups [8]. So in the thermal conversion process MCTP-80 as the thermal conversion temperature increases, the polymerization reaction dominates and short-ring aromatics condense into thick-ring aromatics, so the number of aromatic hydrocarbon rings in the products increases.

3.4 Raman analysis of MCTP-80 and thermal transformation products

The carbon microcrystal content of the thermal conversion products of MCTP-80 at different reaction temperatures was analyzed by Raman spectroscopy. As Fig. 4a shows the Raman spectra of the samples, both MCTP-80 and thermal transformation products have similar Raman peaks. There are two distinct and independent peaks at around 1380 cm^{-1} and 1580 cm^{-1} , the two peaks are very broad and asymmetric, called D peak and G peak, respectively. D peaks are caused by disordered structures or in-plane defects between carbon microcrystal structures, and G peaks are caused by in-plane stretching vibrations of carbon atom sp^2 hybridization [25], where the intensity and width of the peaks depend on the graphitized carbon of the thermal transformation products. For MCTP-80 and thermal transformation products, the characteristic peaks of highly disordered carbonaceous materials can be hidden due to the overlapping peaks between the D and G bands [26]. Therefore, the hidden peaks of the carbon microcrystal structure in the overlapping region were determined by curve fitting method with reference to the hidden peak positions given in Table 3. The curve-fitting criteria were based on the literature [13, 14, 21, 27]. The Raman spectral curves of the thermal transformation products at each temperature were fitted to five independent peaks, as shown in Fig. 4b for the curve-fitted spectrum of MCTP-80.

Table 4 shows the results of calculating the carbon microcrystal content based on the curve-fitted spectra. $\text{IG}/\text{I}_{\text{total}}$ is the ideal graphite crystal content, $\text{ID1}/\text{I}_{\text{total}}$ is the defective graphite microcrystal content, $\text{ID2}/\text{I}_{\text{total}}$ is the carbon microcrystal structure arrangement, $\text{ID3}/\text{I}_{\text{total}}$ is the amorphous carbon content and $\text{ID4}/\text{I}_{\text{total}}$ is the defective carbon microcrystal content. These five parameters were used as indicators to characterize the carbon microcrystalline structure of the thermal transformation products [22]. From

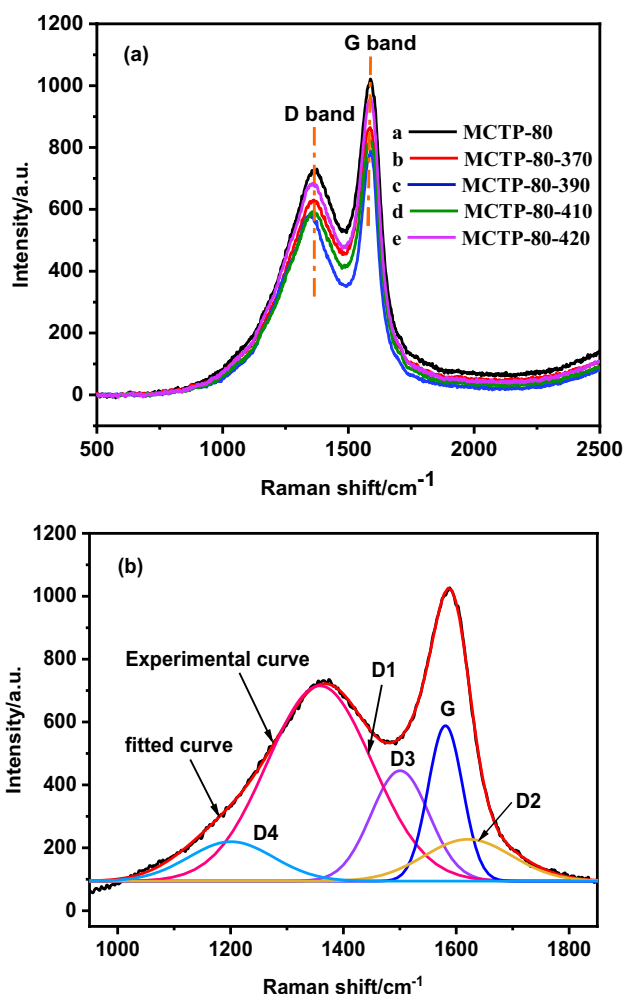


Fig. 4 a Shows the Raman spectrum of the sample b Spectrum of curve fitting results for MCTP-80

Table 4, the $\text{IG}/\text{I}_{\text{total}}$ content of MCTP-80, MCTP-80-370, MCTP-80-390, MCTP-80-410, and MCTP-80-420 gradually increased. Among them, the $\text{IG}/\text{I}_{\text{total}}$ content of MCTP-80-410 and MCTP-80-420 exceeded 20% with 20.17% and 21.86%, respectively. This indicates that they have a high content of ideal microcrystals. As the content of graphitized crystals increases with the increase of thermal transformation temperature, the proportion of G peak area increases and the proportion of defect peak area decreases. $\text{ID1}/\text{I}_{\text{total}}$ is gradually decreasing with increasing thermal transformation temperature, while $\text{ID2}/\text{I}_{\text{total}}$ and $\text{ID4}/\text{I}_{\text{total}}$ are gradually increasing, indicating that the defective microcrystals are transforming each other during the thermal transformation process. The gradual decrease in $\text{ID3}/\text{I}_{\text{total}}$ indicates a decrease in amorphous carbon content. $\text{ID1}/\text{IG}$ is to reflect the degree of ordered and disordered carbon microcrystals, and the content of MCTP-80, MCTP-80-370, MCTP-80-390, MCTP-80-410 and MCTP-80-420 decreases gradually. Among them, the $\text{ID1}/\text{IG}$ of MCTP-80-420 is lower than 2,

Table 3 Raman spectral bands and vibrational modes

| Band | Raman shift (cm ⁻¹) | Vibration mode |
|------|---------------------------------|-----------------------------------------------------------------------------------------|
| G | 1580 | Ideal graphitic lattice (E _{2g} symmetry) |
| D1 | 1350 | Disordered graphitic lattice (graphene layer edges, A _{1g} symmetry) |
| D2 | 1620 | Disordered graphitic lattice (surface graphene layers, E _{2g} symmetry) |
| D3 | 1500 | Amorphous carbon (Gaussian line shape) |
| D4 | 1200 | Disordered graphitic lattice (A _{1g} symmetry), polyenes, and ionic impurities |

Table 4 Calculated Raman spectral parameters of the samples

| Sample | Peak area | | | | | Ratio/% | | | | | |
|-------------|-----------|-------|-------|-------|-------|-----------|------------|------------|------------|------------|--------|
| | ID1 | ID2 | ID3 | ID4 | IG | IG/Itotal | ID1/Itotal | ID2/Itotal | ID3/Itotal | ID4/Itotal | ID1/IG |
| MCTP-80 | 145259 | 25858 | 44252 | 23669 | 38074 | 13.42 | 52.41 | 9.33 | 15.97 | 8.54 | 3.81 |
| MCTP-80-370 | 129209 | 35616 | 32640 | 23826 | 40997 | 15.63 | 49.26 | 13.58 | 12.44 | 9.08 | 3.15 |
| MCTP-80-390 | 109388 | 34664 | 26631 | 27470 | 44110 | 18.25 | 45.26 | 14.09 | 11.02 | 11.36 | 2.17 |
| MCTP-80-410 | 118116 | 40151 | 20771 | 30945 | 52720 | 20.78 | 43.40 | 15.43 | 8.19 | 12.19 | 2.08 |
| MCTP-80-420 | 87998 | 37111 | 15069 | 32122 | 48223 | 21.86 | 39.90 | 16.83 | 6.83 | 14.57 | 1.82 |

indicating that the carbon microcrystals are growing and changing from disordered to ordered structure with a more ordered crystal structure [28].

The above results show that as the reaction degree deepens with the increase of thermal transformation temperature, the disordered structure of carbon microcrystals can be turned into an ordered arrangement so that the planarity becomes higher, the effect of mutual stacking between layers is good, and the intermediate phase microcrystalline components formed by the solidification of the system increase, and the aromaticity is higher, which makes the solid structure of thermal transformation products more stable.

3.5 XRD analysis of MCTP-80 and thermal transformation products

The XRD spectra of MCTP-80 and thermal conversion products are shown in Fig. 5a. It can be seen from the figure that MCTP-80 shows a sharp diffraction peak near $2\theta = 26^\circ$ after polymerization during thermal transformation, which belongs to the graphite (002) surface diffraction peak. This indicates that MCTP-80 has a more perfect crystal structure after polymerization. (002) peak is the superposition of the γ -band (near 20°) and the π -band (near 26°). From the figure, it can be seen that (002) peaks have similar trends and (002) peaks are all asymmetrical broad peaks [17, 20]. However, the difference between the peaks of MCTP-80 and MCTP-80-420 is large. The π -peak of MCTP-80 is completely diffuse, while the π -peak of MCTP-80-420 is sharp and the intensity of the peak is large. This indicates that the thermal transformation product MCTP-80-420 has a higher

degree of interunit structural connectivity in its molecular structure. It indicates that with the increase of thermal transformation temperature, the intermolecular structure is more stable and the aromatic sheet stacking is better regularized, while the number of molecular ring layers is high and the content of aromatic substances increases [16].

XRD combined with the curve fitting method as an important tool to determine the structure of carbon microcrystals, the criteria for curve fitting are based on the literature [16–18, 25]. The fitted curves are shown in Fig. 5b. There are several parameter indicators to determine the carbon microcrystallinity as follows: ideal graphite (I_g), lateral dimensions (L_c), crystal structure layer spacing (d_{002}), number of parallel layers (N) and average number of aromatic rings per layer (n). The crystal structure layer spacing d_{002} was calculated by Bragg Eq. (3), and the other parameters were calculated as (4) to (7), based on the literature [17, 29].

$$d_{002} = \lambda / 2 \sin \theta_{\pi}, \quad (3)$$

$$I_g = A_{\pi} / (A_{\pi} + A_{\gamma}), \quad (4)$$

$$L_c = 0.89 \lambda / \beta_{\pi} \cos \theta_{\pi}, \quad (5)$$

$$N = 1 + L_c / d_{002}, \quad (6)$$

$$n = 0.32 N^2. \quad (7)$$

In the formula, θ_{π} is the diffraction angle of π -peak, λ is the wavelength of X-rays, A_{π} and A_{γ} denote the curve-fitting

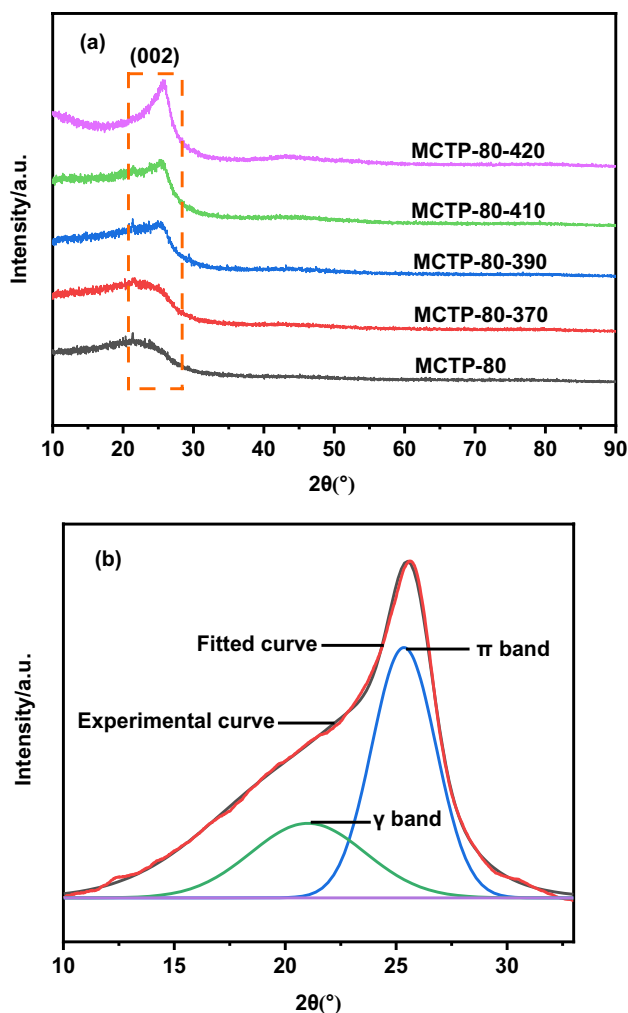


Fig. 5 **a** XRD spectrum of the sample, **b** is the curve fit of MCTP-80

integral area of π -peak and γ -peak, respectively, and β_{π} is the half-peak width of π -peak.

Table 5 shows the relevant microcrystalline parameters of the samples. d_{002} and L_c are important factors affecting the size, stiffness and regularity of the pitch molecular planes. Therefore, the molecular order of MCTP-80 and thermal transformation products can be accurately assessed by d_{002} and L_c . The d_{002} values of MCTP-80, MCTP-80-370, MCTP-80-390, MCTP-80-410, and MCTP-80-420 gradually decreased to 0.3478, 0.3474, 0.3472, 0.3468, and 0.3467,

respectively, while the values of L_c increased to 1.05, 1.26, 1.58, 1.73, and 2.39, respectively. This indicates that the molecular cluster stacking becomes more ordered [30], and the carbon microcrystals of the thermal transformation products become more regularly arranged as the temperature increases. It can be seen from Table 5 that the content of I_g , N and n increased from MCTP-80 to MCTP-80-420. It shows that with the increase of temperature, the graphitization of the products increases, the content of carbon microcrystals increases, and the number of aromatic rings increases, which facilitates the formation of high-quality carbon materials. The above analysis shows that the results of the analytical parameters of XRD are consistent with the analysis of Raman spectroscopy.

3.6 SEM analysis of thermal transformation products

The SEM analysis results of MCTP-80 after thermal transformation products are given in Fig. 6b. From Fig. 6a, it can be seen that the structure of the thermal transformation product MCTP-80-370 shows scattered small spheres, which are mainly composed of aromatic molecules. Figure 6(b) shows the structural morphology of the thermal transformation product MCTP-80-390 in which a large number of small homogeneous spheres start to appear. At this time, the content of aromatic hydrocarbons increased, and the content of carbon microcrystals also increased. As the thermal transformation temperature increases the small spheres begin to melt, and at 420 °C the small spheres disappear and melt, tending to coke development. From the morphology of the four thermal transformation products, MCTP-80-370, MCTP-80-390, MCTP-80-410 and MCTP-80-420, the thermal transformation temperature is between 390 and 420 °C, which is a suitable raw material for preparing high-quality carbon materials.

4 Conclusion

(1) For the preparation of high-quality charcoal materials, MCTP-80 was used as a raw material for this thermal conversion study. I_{ar} and CH_3/CH_2 were calculated using FTIR spectroscopy combined with the mathematical method of

Table 5 Relevant microcrystalline parameters of the samples

| Sample | $\gamma/^\circ$ | $\pi/^\circ$ | A_γ | A_π | $I_g/\%$ | L_c/nm | d_{002} | N | n |
|-------------|-----------------|--------------|------------|----------|----------|-----------------|-----------|------|-------|
| MCTP-80 | 21.57 | 25.59 | 1367.792 | 1256.762 | 47.88 | 1.05 | 0.3478 | 4.03 | 5.21 |
| MCTP-80-370 | 21.13 | 25.62 | 1728.529 | 1685.119 | 49.36 | 1.26 | 0.3474 | 4.62 | 6.82 |
| MCTP-80-390 | 21.66 | 25.63 | 1222.842 | 1957.996 | 61.56 | 1.58 | 0.3472 | 5.55 | 9.84 |
| MCTP-80-410 | 21.49 | 25.66 | 1220.945 | 2202.473 | 64.34 | 1.73 | 0.3468 | 5.99 | 11.48 |
| MCTP-80-420 | 21.06 | 25.68 | 1094.767 | 2163.744 | 66.40 | 2.06 | 0.3467 | 6.99 | 15.49 |

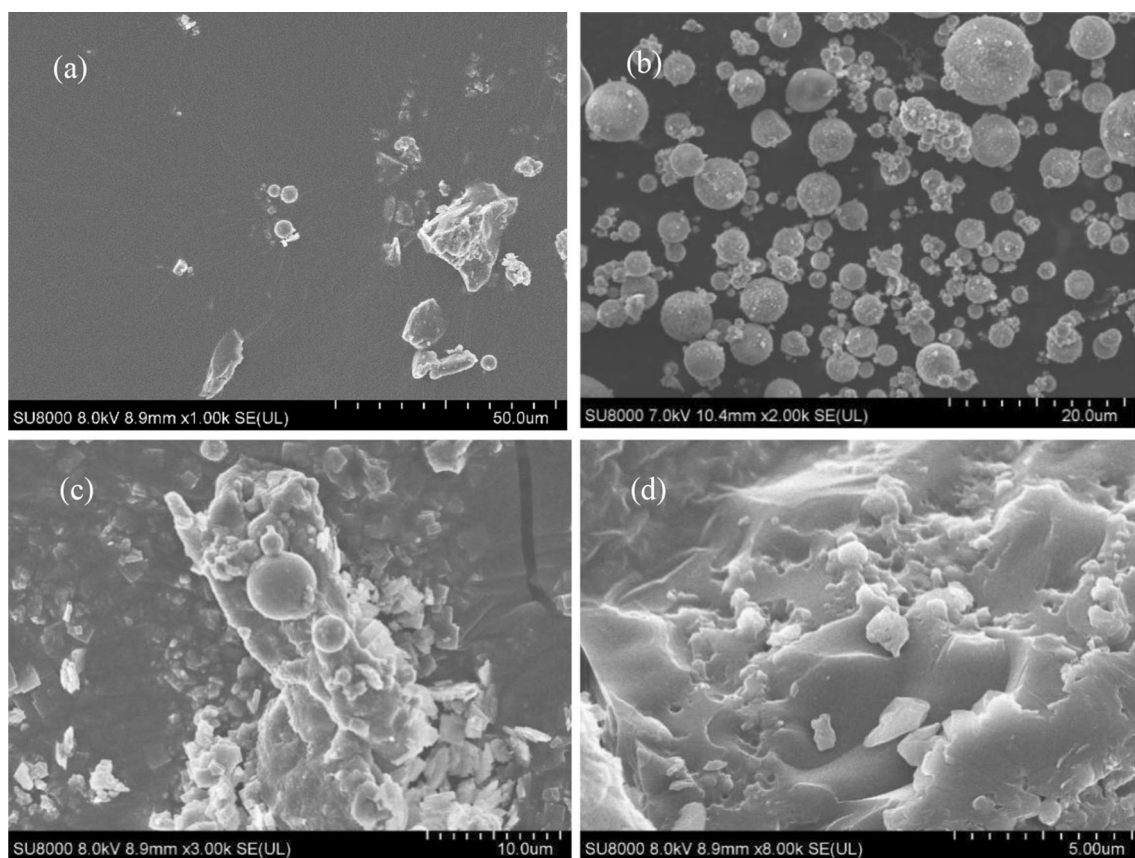


Fig. 6 SEM image of thermal transformation products, **a** MCTP-80-370, **b** MCTP-80-390, **c** MCTP-80-410, **d** MCTP-80-420

split-peak fitting, and it was found that their contents gradually increased with the increase of temperature. The C–O bond introduced by the ethylene tar in MCTP-80 induces the occurrence of a polycondensation reaction in which the C–O bond breaks into a C–C bond. And during the thermal conversion process C–O and C–H functional groups react as reactive sites, resulting in an increase in C–C bonds in the thermal conversion products, an increase in polycyclic aromatic hydrocarbon compounds in the pitch system, and an increase in aromatic content.

(2) The microstructures of MCTP-80, MCTP-80-370, MCTP-80-390, MCTP-80-410, and MCTP-80-420 differed considerably. Conversion of the isotropic pitch in the system to anisotropic pitch when the reaction temperature exceeds 390 °C. When the thermal transformation temperature exceeds 410 °C, the anisotropic spheres in the system start to grow and melt, forming a basin or mosaic structure.

(3) The content of carbon microcrystals and the degree of alignment of the thermal transformation products at different reaction temperatures have a great influence. The carbon microcrystal content of MCTP-80, MCTP-80-370, MCTP-80-390, MCTP-80-410 and MCTP-80-420 was gradually increasing with the increase in reaction temperature. The

addition of ethylene tar and anthracene oil made the thermal conversion products easier to graphitize, and the carbon microcrystal arrangement of the products increased in regularity, resulting in an increase in the aromatic compound content of the thermal conversion products. Therefore, controlling the thermal conversion temperature of MCTP-80 enables the preparation of high-quality carbon materials.

Acknowledgements This work was partially supported by the “Research on Integrated Utilization of Ethylene Tar in Fushun Petrochemical” (LJKZ0409), Liaoning Provincial Department of Education 2021 Scientific Research Project (Surface Project).

Declarations

Conflict of interest The authors declare that they have no conflict of interests.

References

- Perez M, Granda M, Santamaria R (2004) A thermoanalytical study of the co-pyrolysis of coal-tar pitch and petroleum pitch. *Fuel* 83(9):1257–1265. <https://doi.org/10.1016/j.fuel.2003.11.012>

- Ciesińska W (2017) Thermo-rheological properties of coal-tar pitch modified with phenol-formaldehyde resin. *J Therm Anal Calorim* 130(1):187–195. <https://doi.org/10.1007/s10973-017-6471->
- Marković V (1987) Use of coal tar pitch in carbon-carbon composites. *Fuel* 66(11):1512–1515. [https://doi.org/10.1016/0016-2361\(87\)90008-1](https://doi.org/10.1016/0016-2361(87)90008-1)
- Montes-Morán MA, Crespo JL, Young RJ, García R, Moinelo SR (2002) Mesophase from a coal tar pitch: a Raman spectroscopy study. *Fuel Process Technol* 77:207–212. [https://doi.org/10.1016/S0378-3820\(02\)00079-6](https://doi.org/10.1016/S0378-3820(02)00079-6)
- Lin Q, Su W, Xie Y (2009) Effect of rosin to coal-tar pitch on carbonization behavior and optical texture of resultant semi-cokes. *J Anal Appl Pyrol* 86(1):8–13. <https://doi.org/10.1016/j.jaap.2009.03.001>
- Liang ZW, Lu YG, Sun ZL, Luo H (2020) Polymerization kinetics and control of the components of a mesophase pitch. *New Carbon Mater* 35(5):591–598. [https://doi.org/10.1016/S1872-5805\(20\)60512-1](https://doi.org/10.1016/S1872-5805(20)60512-1)
- Tian Y, Huang Y, Yu X, Gao F, Gao S, Wang F, Liu J (2021) Co-carbonization of medium- and low-temperature coal tar pitch and coal-based hydrogenated diesel oil prepare mesophase pitch for needle coke precursor. *Adv Eng Mater* 23(10):2001523. <https://doi.org/10.1002/adem.202001523>
- Zhu Y, Hu C, Zhao C, Xu Y, Gao L, Zhao X (2019) Thermal conversion behavior of medium–low-temperature coal tar pitch during liquid-phase carbonization process. *Chem Select* 4(40):11886–11892. <https://doi.org/10.1002/slct.201902397>
- Tao Y, Liu B, Yan S, Zhaokun M, Huaihe S, Zhanjun L (2019) Thermal transformation behavior of high-temperature coal bitumen intermediate phase. *New Carbon Mater* 34(6):546–551. <https://doi.org/10.19869/j.ncm.1007-8827.2019.06.002>
- Zhu Y, Zhao X, Yuan J, Zhao C, Hu C (2019) Changes in structure of coal liquefied pitch during liquid-phase carbonization process. *Carbon Lett* 29(1):37–45. <https://doi.org/10.1007/s42823-019-00016-0>
- Zhao CL, Zhu YM, Gao LJ, Cheng JX, Lai SQ, Zhao XF (2021) Oxidative modification of ethylene residue asphalt and its thermal conversion behavior. *Adv Chem Eng* 40(4):2130–2137. <https://doi.org/10.16085/j.issn.1000-6613.2020-1012>
- Zhu YM, Zhao XF, Gao LJ, Cheng JX (2018) FTIR peak splitting fitting method to quantify structural changes during thermal conversion of refined coal bitumen. *Spectrosc Spectr Anal* 37(7):2076–2080. [https://doi.org/10.3964/j.issn.1000-0593\(2018\)07-2076-05](https://doi.org/10.3964/j.issn.1000-0593(2018)07-2076-05)
- Sadezky A, Muckenhuber H, Grothe H, Niessner R, Pöschl U (2005) Raman microspectroscopy of soot and related carbonaceous materials: spectral analysis and structural information. *Carbon* 43(8):1731–1742. <https://doi.org/10.1016/j.carbon.2005.02.018>
- He X, Liu X, Nie B, Song D (2017) FTIR and Raman spectroscopy characterization of functional groups in various rank coals. *Fuel* 206:555–563. <https://doi.org/10.1016/j.fuel.2017.05.101>
- Pawlyta M, Rouzaud JN, Duber S (2015) Raman microspectroscopy characterization of carbon blacks: spectral analysis and structural information. *Carbon* 84:479–490. <https://doi.org/10.1016/j.carbon.2014.12.030>
- Zhu Y, Zhao C, Xu Y, Hu C, Zhao X (2019) Preparation and characterization of coal pitch-based needle coke (Part I): the effects of aromatic index (fa) in refined coal pitch. *Energy Fuels* 33(4):3456–3464. <https://doi.org/10.1021/acs.energyfuels.9b00160>
- Zhu YM, Zhao XF, Gao LJ, Cheng JX, Lv J, Lai SQ (2017) Quantitative study of XRD and Raman peak splitting fitting of the microcrystalline structure of coal-based needle coke. *Spectrosc Spectr Anal* 37(6):1919–1924. [https://doi.org/10.3964/j.issn.1000-0593\(2017\)06-1919-06](https://doi.org/10.3964/j.issn.1000-0593(2017)06-1919-06)
- Qin F, Jiang W, Ni G, Wang J, Zuo P, Qu S, Shen W (2019) From coal-heavy oil co-refining residue to asphaltene-based functional carbon materials. *ACS Sustain Chem Eng* 7(4):4523–4531. <https://doi.org/10.1021/acssuschemeng.9b00003>
- Meyer zu Reckenderf R (1996) Analysis of coal-tar pitches. *Fuel Energy Abstr* 37(4):309. [https://doi.org/10.1016/0140-6701\(96\)82753-6](https://doi.org/10.1016/0140-6701(96)82753-6)
- Lv J, Bai H, Zhu Y, Hu C, Xu Y, Lai S, Zhao X (2021) Synthesis and characterization of mesophase coke from medium–low-temperature coal tar pitch modified by high-pressure thermal polymerization. *Asia-Pac J Chem Eng* 16(4):e2643. <https://doi.org/10.1002/apj.2643>
- Zhu Y, Xu Y, Hu C, Yin X, Zhao C, Gao L, Zhao X (2019) Preparation and characterization of mosaic coke from heavy-phase coal pitch. *Asia-Pac J Chem Eng* 14(6):e2369. <https://doi.org/10.1002/apj.2369>
- Meng F, Yu J, Tahmasebi A, Han Y, Zhao H, Lucas J, Wall T (2014) Characteristics of chars from low temperature pyrolysis of lignite. *Energy Fuel* 28:275–284. <https://doi.org/10.1021/ef401423s>
- Ibarra J, Munoz E, Moliner R (1996) FTIR study of the evolution of coal structure during the coalification process. *Organic Geochem* 24(6–7):725–735. [https://doi.org/10.1016/0146-6380\(96\)00063-0](https://doi.org/10.1016/0146-6380(96)00063-0)
- Yen TF, Wu WH, Chilingar GV (1984) A study of the structure of petroleum asphaltene and related substances by infrared spectroscopy. *Energy Sour* 7(3):203–235. <https://doi.org/10.1080/00908318408908084>
- Beysac O, Goffé B, Petitet JP, Froigneux E, Moreau M, Rouzaud JN (2003) On the characterization of disordered and heterogeneous carbonaceous materials by Raman spectroscopy. *Spectrochim Acta Part A Mol Biomol Spectrosc* 59(10):2267–2276. [https://doi.org/10.1016/S1386-1425\(03\)00070-2](https://doi.org/10.1016/S1386-1425(03)00070-2)
- Ulyanova EV, Molchanov AN, Prokhorov IY, Grinyov VG (2014) Fine structure of Raman spectra in coals of different rank. *Int J Coal Geol* 121:37–43. <https://doi.org/10.1016/j.coal.2013.10.014>
- Morga R, Jelonek I, Kruszewska K (2014) Relationship between coking coal quality and its micro-Raman spectral characteristics. *Int J Coal Geol* 134:17–23. <https://doi.org/10.1016/j.coal.2014.09.013>
- Chen MH, Li M (2021) Progress in the preparation and characterization of intermediate phase asphalt. *Carbon Technol* 40(4):6. <https://doi.org/10.14078/j.cnki.1001-3741.2021.04.001>
- Chun-Ting D, Liu Jun-Qing X, Wen-Qiang LP, Dong-Fang Z, Qiu-Shi W, Huai-He S (2018) Characterization of intermediate phase asphalt from three different raw materials. *Chem Progress* 37(01):189–194. <https://doi.org/10.16085/j.issn.1000-6613.2017-0789>
- Lee S, Eom Y, Kim BJ, Mochida I, Yoon SH, Kim BC (2015) The thermotropic liquid crystalline behavior of mesophase pitches with different chemical structures. *Carbon* 81:694–701. <https://doi.org/10.1016/j.carbon.2014.10.007>

Publisher's Note Springer Nature remains neutral with regard to jurisdictional claims in published maps and institutional affiliations.

Springer Nature or its licensor (e.g. a society or other partner) holds exclusive rights to this article under a publishing agreement with the author(s) or other rightsholder(s); author self-archiving of the accepted manuscript version of this article is solely governed by the terms of such publishing agreement and applicable law.